Cement and Concrete Research 39 (2009) 779–786

Contents lists available at ScienceDirect

Cement and Concrete Research

journal homepage: http://ees.elsevier.com/CEMCON/default.asp

Characterising the time-dependant behaviour on the single fibre level of SHCC: Part 1: Mechanism of fibre pull-out creep

William P. Boshoff [a,*], Viktor Mechtcherine [b], Gideon P.A.G. van Zijl [c,d]

[a] Division for Structural Engineering, University of Stellenbosch, Private Bag X1, Stellenbosch, South Africa
[b] Faculty of Civil Engineering, TU Dresden, Germany
[c] Division for Structural Engineering, University of Stellenbosch, South Africa
[d] Faculty of Architecture, Delft University of Technology, The Netherlands

ARTICLE INFO

Article history:
Received 1 June 2008
Accepted 8 June 2009

Keywords:
Creep
Fibre reinforcement
Tensile properties
Shrinkage
Fibre pull-out

ABSTRACT

SHCC (Strain Hardening Cement-based Composite) has been designed and optimised to overcome the main weaknesses of ordinary concrete, which is its brittleness. SHCC shows a high tensile ductility and can resist the full load at a tensile strain of more than 4%. An in depth investigation into the time-dependant behaviour is still lacking for SHCC. This paper is the first part of a two paper series about the time-dependant behaviour on the single fibre level. In this paper, the tensile creep behaviour of SHCC is studied to distinguish mechanisms of creep. Tensile creep and shrinkage test results are reported for dumbbell type SHCC specimens. The specimens are pre-cracked to simulate in-service conditions, with subsequent sustained load at various levels, here chosen as 30%, 50%, 70% and 80% of the ultimate resistance. To distinguish the sources of significant creep deformation under these sustained loads, single fibre pull-out tests are performed under sustained load. It is shown that the time-dependent fibre pull-out is a significant source of time-dependent deformation, along with the formation of new cracks in SHCC under sustained load.

1. Introduction

In the quest for more durable building materials, SHCC (Strain Hardening Cement-based Composites) have been developed over the past decade and half and have become a promising alternative for traditional building materials [1,2,4]. SHCC has superior qualities in terms of ductility under tensile loading, with a tensile strain capacity of more than 3%. This strain capacity is in the same order as that of reinforcing steel and hence strain compatibility is ensured when SHCC is reinforced [3].

Another important advantage of SHCC is the multiple cracking during tensile loading [1–2]. The cracks are usually less than 100 μm in width [1] and do not widen significantly during the strain hardening phase. This leads to improved durability performance of a steel reinforced SHCC structure compared to ordinary steel reinforced concrete [5]. Intensive research is currently undertaken internationally to characterise the durability performance of SHCC. However, the positive effect of narrow cracks can be only maintained if the cracks do not widen significantly under a sustained load which would invalidate the improved durability if the cracks open wider than some threshold value.

The time-dependant behaviour of SHCC has only recently received attention. Maalej et al. [6] and Boshoff and Van Zijl [7] showed that the ductility is not affected by the strain rate. However, Maalej et al. [6] demonstrated that there is a strong increase of the ultimate tensile strength with an increase of strain rate. The rate effect was further investigated on the single fibre level [10] and it was found that a pronounced rate effect is present with regard to the pull-out resistance of single fibres embedded in the matrix. However, no such strong rate effect was observed on the macro-level, since the failure mechanism of the fibres change from pull-out at low rates to fibre rupture at high rates [10].

An important phenomenon that was identified by Boshoff and Van Zijl [7] is that during a sustained tensile load, more cracks can initiate and that the tensile creep rate and magnitude increase after SHCC has cracked. These issues are further investigated in this paper and light is shed on the source of these time-dependant phenomena. This was done by monitoring the tensile creep strain of SHCC specimens after they were pre-damaged to simulate cracked SHCC. An increase of creep strain rate was found and the source of this creep, which causes widening of cracks, was further investigated by performing single fibre pull-out creep tests.

2. Experimental program

The experimental program to investigate the source of the tensile creep behaviour of cracked SHCC consisted out of three parts. Firstly, tensile creep tests were performed on cracked specimens at different load levels to investigate the influence of cracks on the development

* Corresponding author.
E-mail address: bboshoff@sun.ac.za (W.P. Boshoff).

0008-8846/$ – see front matter © 2009 Elsevier Ltd. All rights reserved.
doi:10.1016/j.cemconres.2009.06.007

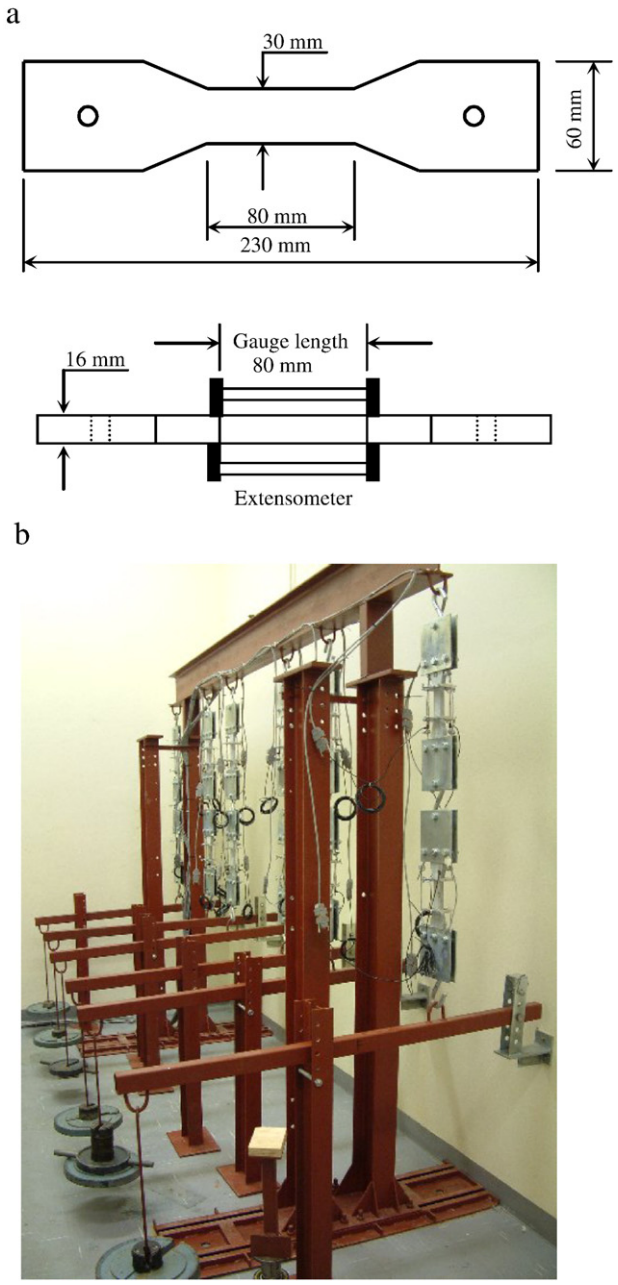

Fig. 1. a) The dimensions of the tensile specimens for the creep tests. b) The tensile creep frame.

of creep deformations. Secondly, pull-out creep tests were done on single fibres embedded in the SHCC matrix. Lastly, creep tests were carried out on single fibres to find the influence of fibre creep on the time-dependant behaviour of SHCC. Note that creep tests on the uncracked matrix have already been performed in earlier investigations [7].

The same mix proportions were used for all the tests. The water/binder ratio was 0.4 and the aggregate/binder ratio was 0.5. The binder consisted of CEM I 42.5 cement, a fly ash extender marketed as PozzFill by Ash Resources, South Africa, and Corex Slag of origin of the Saldanha Steel Refinery in the Western Cape Province, South Africa used in the ratio of 45:50:5 by mass, respectively. Fine sand with a maximum particle size of 210 μm was used. For the tests on the SHCC specimens, PVA (Polyvinyl Alcohol) fibres with a length of 12 mm and a 40 μm diameter were added at 2% by volume. A super plasticiser and a viscosity modification agent were used to adjust the rheological behaviour of the mixture.

After casting, the moulds were taken to a temperature controlled room at 23 °C. The specimens were cured in the closed moulds for 72 h before they were stripped. The specimens were then submerged in clean potable water at 23 °C until an age of 13 days. Sikagard 63N, a brush applied sealant supplied by Sika SA, was used to seal the specimens directly after they were taken out of the water to minimise the effect of drying shrinkage during the testing. All specimens were then tested at an age of 14 days. It is acknowledged that the matrix cracks that arose during the pre-cracking of the specimens may have broken the seal, but the rate of drying would still be reduced.

2.1. Creep of pre-cracked specimens

The true benefit of SHCC is only utilised after the material has cracked. The creep of cracked SHCC is thus important as it would be the condition of SHCC in its intended use. For this reason, tensile creep tests were performed on SHCC specimens that were pre-cracked under controlled conditions before the tensile creep load was applied.

The creep test setup was designed and built to apply the creep load with free hanging weights acting on the specimens with a lever arm. The load was applied to two specimens in series. Fig. 1 shows the dimensions of the specimens and the test setup. Two LVDT's were fixed to an aluminium frame that was clamped over the gauge length to measure the strain of each specimen, cf. Fig. 1a. The climate room where the tests were performed was controlled to be at a constant temperature of 23 ± 1 °C and a relative humidity of 65 ± 5%.

The pre-cracking occurred in a Zwick Z250 testing machine using the same test setup as described in Boshoff and Van Zijl [7] for tensile tests. The specimens were subjected to a direct tensile load up to a level of 1% strain at a strain rate of 0.1 mm/s and then unloaded at the same rate. The specimens were then fixed in the creep setup and loaded with the sustained load within an hour after the cracking.

Four different load levels were tested using two specimens for each test, as shown in Table 1. Two specimens per loading level are not enough to accurately quantify the creep response due to possible experimental scatter, but the results will nevertheless give a good indication of the effect of the loading level on the magnitude and rate of creep. Potential tensile creep fracture is also investigated as the possibility exists that the specimens at the higher sustained load could fail in time.

Photos were taken of the specimens after they were pre-cracked before the creep load was applied and again periodically during the creep tests. These photos are not of sufficient resolution to distinguish all the cracks or crack sizes. Note also that these specimens were sealed which further complicates the crack visualisation and quantification. These photos do however give an indication of how the damage evolved during the creep tests since the widening of cracks was distinguishable.

Four trial pre-cracking tests were performed in the Zwick Z250 testing machine to study the consistency of the unloading response. Fig. 2 shows the reasonably consistent unloading response of the SHCC specimens. Note that reloading was also included in the trial tests. For the creep tests, the pre-cracked specimens were removed from the Zwick Z250 after loading to 1% strain and subsequent unloading. They were then taken to the creep frame and reloaded to the respective sustained load levels. These load levels are shown in dashed lines

Table 1
Test program for the cracked creep specimens.

Loading as % of the tensile strength	30%	50%	70%	80%
Actual applied stress [MPa]	0.81	1.32	1.87	2.11

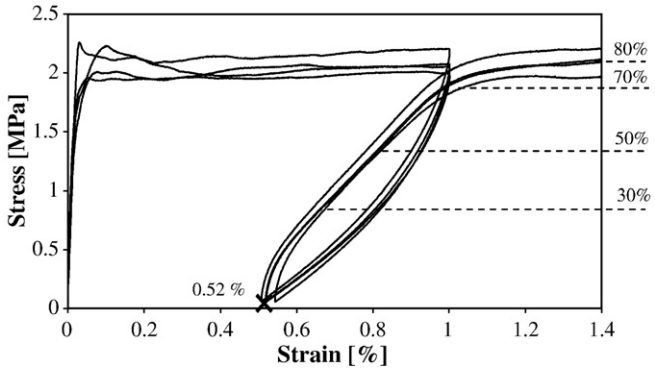

Fig. 2. Trial pre-cracking tests with unloading after reaching 1% tensile strain. Note that the actual pre-cracking did not include the re-loading shown here for the trial tests. The sustained stress levels in the subsequent creep tests are shown in dashed lines.

in Fig. 2. For the trial tests, as well as the pre-cracking of the creep specimens the Zwick cross head speed was kept constant at 0.1 mm/s.

2.2. Fibre pull-out creep tests

To study a potential dominant source of the tensile creep behaviour found for the SHCC specimens (macro level), creep tests were performed on single fibres (micro level). A sustained load was applied to single fibres individually which were embedded in the matrix at a specific embedment length.

The matrix used was the same as for the SHCC specimens described in Section 2.1 except that no fibres were added to the mix. The specimens for the production of test samples were cast following Katz and Li [11]. The casting mould is shown in Fig. 3a. The fibres are drawn in for illustration purposes as they are too fine to be seen on the photo.

After casting the mould was wrapped in plastic to ensure no moisture loss during the hardening process and was left in a climate controlled box at 23 °C. The mould was carefully stripped after 24 h and the specimens were submerged in clean potable water at 23 °C until testing. All specimens were tested at the age of 14 days. Moments before the test execution, the specimens were cut from the larger block (Fig. 3b) to the final geometry (Fig. 3c), ensuring the correct embedment lengths.

It is acknowledged that the preparation of the fibre embedment is not entirely representative of a fibre that is embedding during mixing. Differences may occur due to compaction, minor damage to fibres and internal shrinkage. While these three aspects may still complicate accurate modelling of the mechanisms of time-dependence of SHCC based on the single fibre test data, they do not invalidate the findings on the significance of the mechanisms.

The test setup for the single fibre pull-out tests is based on the test setup of Kanda and Li (1998) and a schematic representation is shown in Fig. 4. A Schenk 250 kN Universal Testing Machine was used for the tests. A 10 N load cell (HBM) was mounted on the top crosshead with a fibre gluing plate fixed to the load cell. On the bottom platen a base plate was fixed onto which the test sample was glued. The specimen was glued to the bottom base plate using a two component glue, X60 supplied by HBM. Special care was taken to ensure that no glue came in contact with the end of the embedded fibre as it could influence the pull-out force. The loose end of the fibre was carefully glued to the fibre mounting plate with a "superglue" type Z70 also supplied by HBM. This was all done while ensuring that no force was applied to the fibre that could cause debonding or pull-out. The force was monitored during the gluing process and if a force was applied that could have damaged the test sample, the results of that test were disregarded. A microscope was used to ensure that the gluing process was executed successfully. A gap of about 1 mm was ensured between the bottom of the fibre mounting plate and the test sample.

The displacement during this creep test was measured optically using a microscope with a 1 Mega-pixel camera. Photos were taken at given intervals and were used to obtain the pull-out displacement by scaling. The thickness of the fibre, i.e., 40 μm, was used as a scale reference. Fig. 5 shows an example of such measurements.

Two sets of creep tests were performed. For one set the sustained creep load was applied to the fibres. For another set the fibres were debonded from the matrix before the creep load was introduced. The debonding was achieved by pulling the fibre with a constant pull-out rate from the matrix using the actuator until a slight load drop or change of gradient occurred in the force-displacement response, which indicated that the fibre was debonded completely. Table 2 gives the actual initial embedment lengths for each test.

Three tests of each set were performed with sustained load causing an average fibre-matrix interfacial shear stress of 1.2 MPa, which is

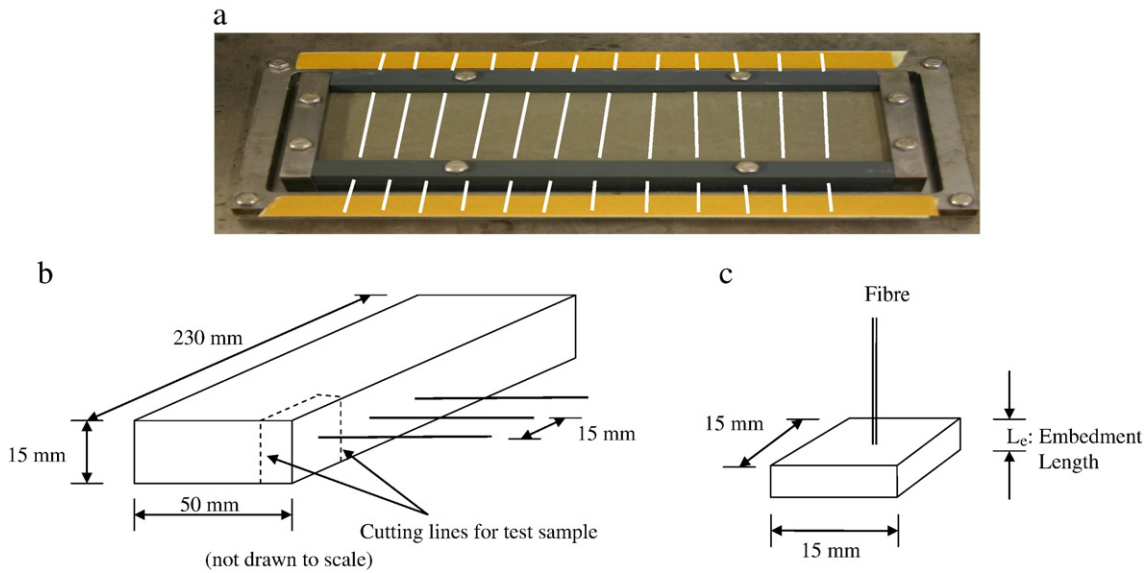

Fig. 3. (a) Steel mould (with fibres drawn in for visibility) for casting a (b) fibre reinforced block from which (c) individual single specimens are cut for the single fibre pull-out tests.

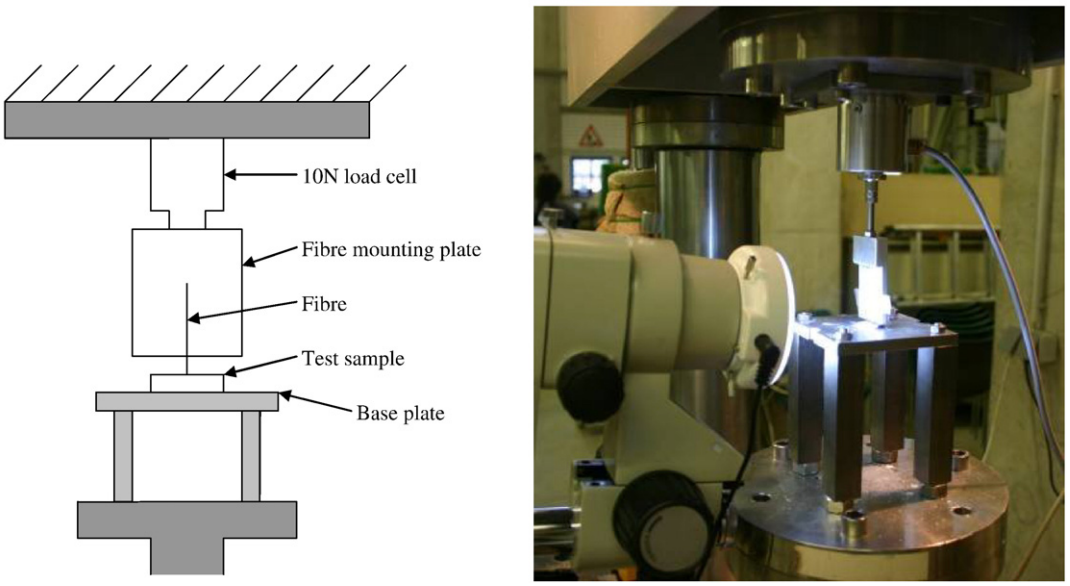

Fig. 4. The single fibre pull-out test setup.

50% of the average shear strength of 2.4 MPa found for these fibres and test setup at a medium testing rate of 1 mm/min in recent tests [8]. The load was kept constant until the fibre was pulled out completely.

2.3. Fibre creep test

A creep test on a single fibre was performed to investigate the possible influence that the creep of the fibre material itself has on the macroscopic behaviour of SHCC when exposed to a sustained tensile load. The fibre creep tests were done with a similar test setup as the time-dependant fibre pull-out tests, except that another fibre mounting plate was fixed to the bottom base plate by gluing. The creep deformation of the fibre was again measured by scaling from the microscope photos.

For the fibre creep test, only one fibre was tested to obtain a rough indication of the fibre creep. The fibre was loaded at 50% of its tensile strength of 1560 MPa. The load was kept constant for a duration of 60 h and photos were taken using the microscope at specific time intervals and used to determine the time-dependant increase of the length of the fibre.

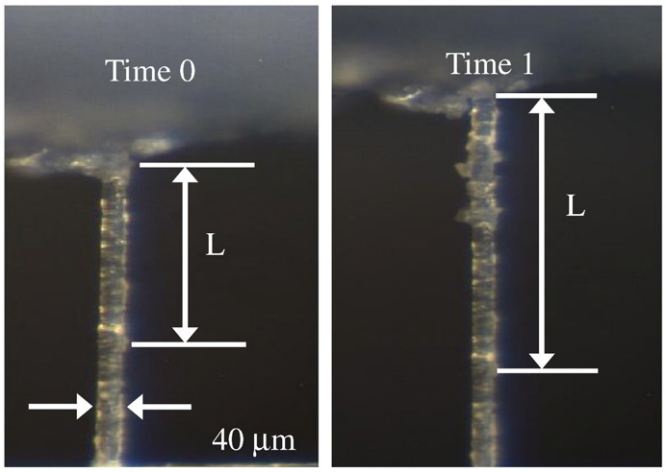

Fig. 5. An example of the fibre pull-out displacement measurement using the microscope photos with the pull-out displacement at Time 1 being the difference between L_0 and L_1. The fibre diameter is used as a scale.

3. Experimental results

3.1. Pre-cracked tensile creep results

The time-dependent strains, i.e., the strains evolving from the moment the respective sustained load levels were reached, are shown in Fig. 6a. Note that the average of the two specimens at each creep load level is shown. Fig. 6b shows the shrinkage strain evolutions, i.e., the time-dependent strains of two unloaded, unsealed specimens kept in the same controlled climate as the creep specimens. By subtraction of the average shrinkage strains from the total time-dependent strains, and normalisation by the creep stress level, the specific creep strains shown in Fig. 6c were computed.

Note that, although the specific creep strains shown in Fig. 6c are indicative of the creep response, they are not accurate, for three main reasons. Firstly, the crack patterns, and thus the total cracked surface differ significantly for the various specimens, with fewer cracks in the specimens subjected to lower sustained loads. The shrinkage specimens were not pre-cracked. Secondly, although the creep specimens were sealed as described in Section 2.1, drying shrinkage is apparent from the time-dependent responses in Fig. 6a. For the 30% tensile creep load, overall shortening occurred, through shrinkage domination. Due to the cracks, the seal was broken and moisture loss and associated shrinkage could occur, although at a lower rate than in the case of an unsealed specimen. Thirdly, due to the simultaneous drying, the time-dependent strains include drying creep, i.e., enlarged strain under sustained load when simultaneous drying occurs.

It is however clear in Fig. 6a that the creep dominates the time-dependant behaviour at higher loading levels.

Fig. 7 shows the strain evolution of selected specimens during the first 5 h. Sudden increase of strain as observed in the experiments indicates that new cracks were formed during the first hours after loading. These jumps in the curve course are encircled in Fig. 7.

In order to rank the measured time-dependant strains they are shown in Fig. 8 in a stress–strain graph together with some

Table 2
Actual embedment lengths in the time-dependant fibre pull-out creep tests.

	Debonded tests			Fully bonded tests		
Actual embedment length [mm]	1.3	1.3	1.4	1.4	1.5	1.35

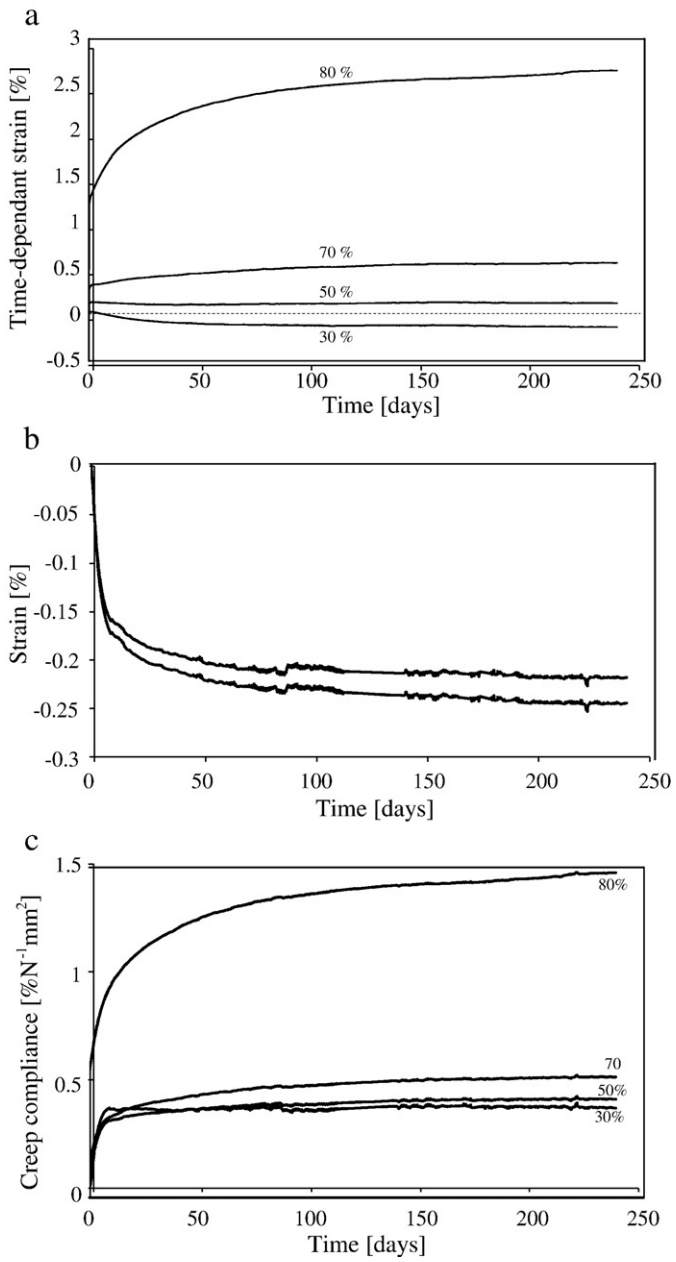

Fig. 6. (a) Average time-dependant strains for each loading level and (b) shrinkage measured on unloaded, unsealed specimens and (c) computed creep strains by subtraction of average shrinkage strains.

representative curves obtained from monotonic tensile tests with various strain rates as reported in Boshoff and Van Zijl [7]. The two specimens of each loading level are marked with triangle and circle indicators, respectively. The points where the creep started after pre-cracking are indicated with a cross. These points were calculated by adding the permanent strain after unloading in the pre-cracking phase, i.e., roughly 0.52% cf. Fig. 2, to the "instant" or mechanical strain recorded during the creep load application. Good agreement is seen between the total strain levels at the onset of the sustained load in Figs. 2 and 6, for the various creep tests.

The total time under sustained load of each indicator is also given in Fig. 8.

The time-dependent strain shown in Fig. 8 is alarmingly high. One of the specimens loaded with an 80% tensile creep load showed stains beyond the softening branches from the tensile test. Nevertheless, creep fracture did not occur for any of the specimens. Even though the

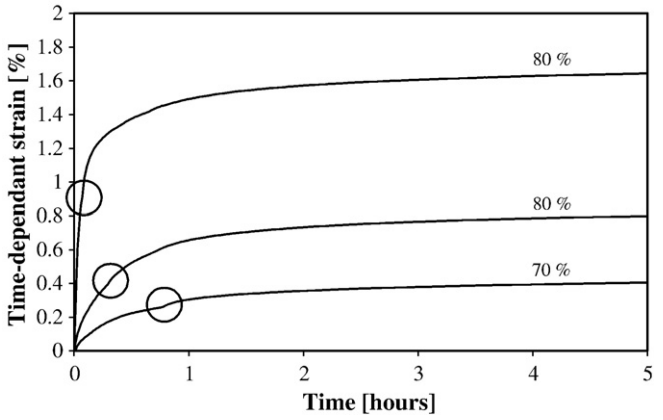

Fig. 7. The time-dependant strain of three individual specimens during the first 5 h of loading with 70% and 80% of the tensile strength, respectively. The marked sudden increases in strain indicate the formation of new crack(s).

monitoring of the strains was stopped after 8 months, the load was sustained on the 80% tensile creep specimens, and after 24 months they had not failed.

3.2. Single fibre pull-out creep tests

Unlike in the above described creep experiments on the SHCC specimens, all the time-dependant fibre pull-out creep tests resulted in failure, i.e., the fibre pulled out of the matrix over a period of time. Fig. 9 gives the time to failure for each set of tests, i.e., debonded and non-debonded fibres, showing the individual as well as the average values.

For the calculation of the pull-out displacement of the fibres the method of using microscope photos was used as described in Section 2. These pull-out displacements are shown in Fig. 10. The failure occurred directly after the last value for each specimen was recorded.

3.3. Single fibre creep

For the fibre creep test, the microscope method was used to determine, in this case, the increase of the length of the fibre over time. For this, two marks were identified on the fibre and the distance between these two marks was measured using the microscope photos over a period of 60 h. Fig. 11 shows the results of these measurements together with a line which indicates what the measured lengths would be if a slight creep (here: 0.5%) would occur linearly over the

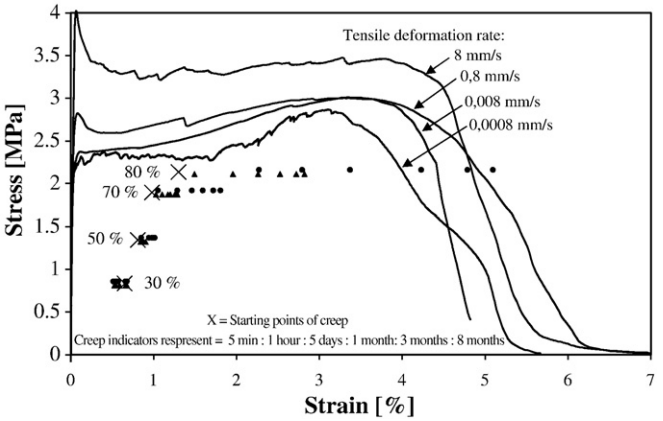

Fig. 8. The time-dependant strains from the creep tests are shown together with representative curves from the monotonic tension tests [7].

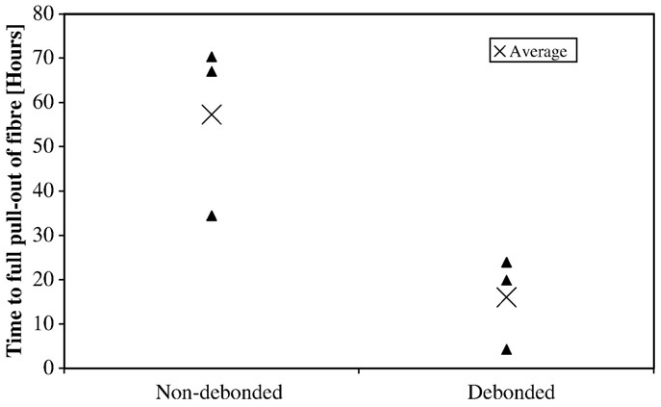

Fig. 9. The time to failure for the time-dependent fibre pull-out creep tests loaded at 50% of the ultimate pull-out resistance.

time period of 60 h. The fibre was loaded at 580 MPa, i.e., half the embedded tensile strength of the fibre.

4. Discussion

4.1. Tensile creep of pre-cracked specimens

All the cracked section creep tests were loaded with a creep load lower than what caused the pre-damage. These tests represent the behaviour of SHCC on which an event like earthquake or extreme live loading occurred, which mobilised the strain hardening capacity of the material, and to which a lower, sustained load was applied afterwards.

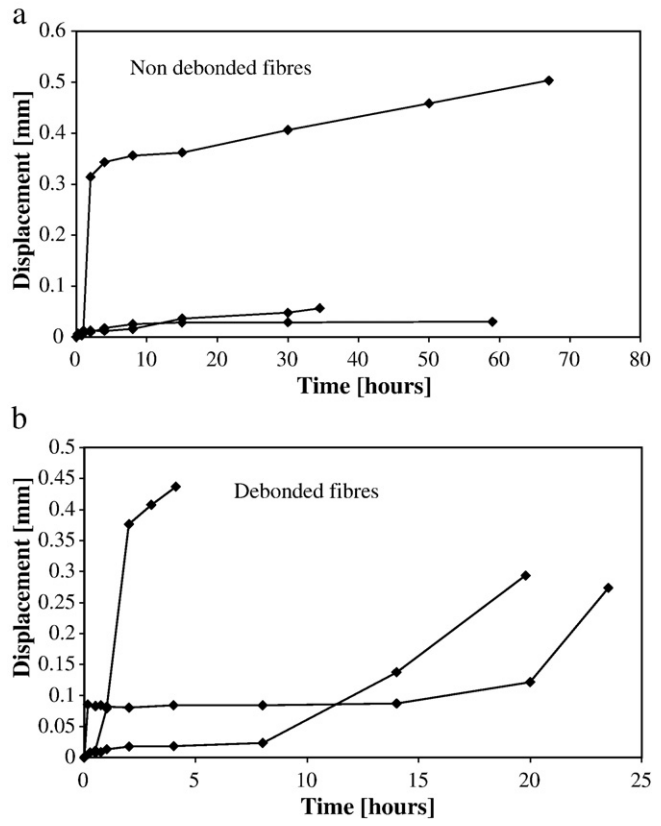

Fig. 10. The fibre pull-out displacements over time shown for the non debonded (a), and debonded fibres (b).

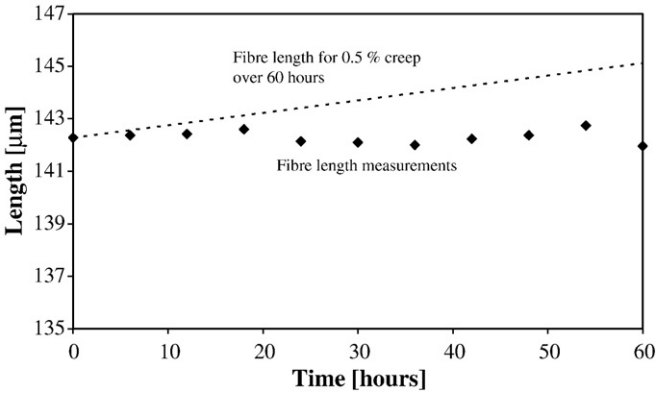

Fig. 11. The length measurement on the fibre during a creep test together with a line indicating what the response would be if a linear creep of 0.5% over 60 h would occur.

To further analyse the results the creep compliance, C_c, was calculated. C_c is defined according to Eq. (1):

$$C_c = \frac{\varepsilon_c}{\sigma} \tag{1}$$

with ε_c the creep strain and σ the applied stress. The average time-dependant strains at the end of the 8 months were considered and a shrinkage strain of 0.23% (Fig. 6b). Fig. 12 shows the calculated C_c values. For a comparison the C_c of the average creep obtained by Boshoff and Van Zijl [7] from the tests on uncracked SHCC specimens is given as well.

It can be seen on Fig. 12 that the creep compliance of cracked specimens is significantly higher than that of uncracked specimens. Furthermore, the creep increases almost exponentially at the higher loads. This increased creep of cracked specimens can only be ascribed to three possible sources, namely the initiation of new cracks, the widening of the existing cracks over time and the creep of fibres bridging the cracks.

Photos of the crack pattern of this specimen (80% tensile creep) are shown at different times under sustained loading in Fig. 13. Crack saturation does not occur. After the pre-cracking up to an average tensile strain of 1%, several cracks were formed. Under the subsequent sustained load, there are indications of new crack formation in the form of sudden increases in the deformation (Fig. 7). By careful inspection of the photos, this is confirmed and the number of cracks increased from 11 at the start of creep, to 17 at 8 months. By consideration of these numbers of cracks, the shrinkage strain (Fig. 6b) and creep strain (Fig. 8) levels for the shown specimen, and assuming viscoelastic matrix behaviour between cracks, the average crack width

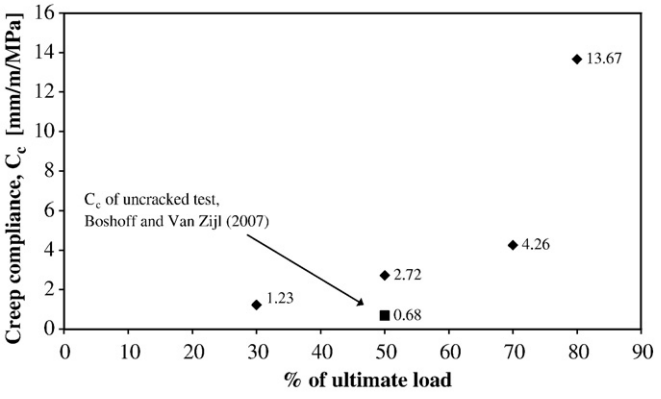

Fig. 12. The creep compliance, C_c, of a cracked section loaded at different levels. The creep value for uncracked SHCC observed by Boshoff and Van Zijl [7] is also indicated.

Fig. 13. Photos taken of one of the pre-cracked tensile creep specimens loaded at 80% of the tensile strength. The time after loading is from left to right: 30 min, 12 h, 6 days and 8 months.

at the onset of creep, and that at 8 months can be estimated to be 78 μm and 244 μm respectively. For this calculation, the concept of decomposition of total strain in elastic (ε_e), creep (ε_e), shrinkage (ε_e) and "cracking" strain (ε_{cr}) was applied as follows:

$$\varepsilon(t) = \varepsilon_e(t) + \varepsilon_c(t) + \varepsilon_s(t) + \varepsilon_{cr}(t) \tag{2}$$

Note also that the time dependence of each strain component in Eq. (2). The "cracking" strain is given by

$$\varepsilon_{cr}(t) = \frac{n_c(t)\overline{w}_c(t)}{L_g} \tag{3}$$

where n_c is the number of cracks in the gauge length (L_g) and $\overline{w}_c$ is the average crack width. Both the number of cracks and the average crack width are functions of time. From Eqs. (2) and (3) the average crack width can be expressed as

$$\overline{w}_c(t) = \left[\varepsilon(t) - \left(\frac{\sigma}{E_c(t)} + C_c(t)\sigma + \varepsilon_s(t)\right)\right]\frac{L_g}{n_c(t)} \tag{4}$$

Note that the average elastic modulus for this SHCC is $E_c = 9.2$ GPa at 14 days [7]. It roughly doubles from this young age to 5 months [9]. A value of 20 GPa was used for the calculation of crack width at 8 months cf. Eq. (4).

Therefore, instead of the formation of evenly spaced cracks over the whole gauge length, only a limited number of new cracks are formed under the sustained load. Crack saturation is not reached, as is clear from Fig. 13. The time-dependent deformation is therefore attributed to new crack formation, matrix creep, as well as crack widening in time.

4.2. Time-dependant fibre pull-out

In Eq. (3) two sources of time dependence of the cracking strain are identified, namely the number of cracks and the crack width. It has been shown in Fig. 13, and argued in the previous section that the number of cracks increases under creep load in time, but also that cracks widen. The widening of each crack can be attributed to fibre creep and fibre pull-out. The single fibre pull-out creep tests address the latter contribution to time-dependent deformation of SHCC. It is alarming that all the fibres tested were pulled out within 70 h at a load corresponding to just 50% of the shear strength of the bond, as reported in Section 3.2. This indicates that the failure due to creep occurs on this small scale.

The average time to pull-out for non-debonded creep tests was 57 h, while for the debonded tests 16 h. This difference shows that after the full debonding of a fibre from the matrix, the resistance to creep deformations reduces significantly. The pull-out displacements of the fibres plotted against time in Fig. 10 display no clear trend for the rate of pull-out at a constant load. A greater number of experiments are needed to quantify any trend if it exists.

However, the single fibre pull-out creep test cannot represent the true conditions in an SHCC material in all their complexity. Firstly, the embedment lengths of the tests were between 1.3 and 1.5 mm while the embedment length in the SHCC matrix under investigation is up to 6 mm, i.e., half the fibre length. Secondly, the fibres were always pulled out parallel to the fibre axis and perpendicular to the sample surface, i.e., the effect of real orientations. Due to these differences, the results of the single fibre pull-out creep tests cannot be used to directly link the creep on the single fibre level to the macro-level. However, the results clearly show that the time-dependant pull-out of fibres is a source of the crack widening over time.

4.3. Fibre creep

To distinguish fibre creep from the pull-out creep deformation, the time-dependent deformation of a single fibre was measured under a sustained normal stress of 580 MPa. This creep load is nearly 5 times the fibre normal stress in the pull-out creep stress. Under these conditions insignificant time-dependent deformation of the fibre was measured. So, the fibre creep does not contribute here to the crack widening phenomenon found under a sustained load. The crack widening phenomena is rather attributed to the time-dependant pull-out of the fibres.

4.4. Mechanisms of SHCC time dependence

By consideration of the terms of Eq. (2), it can be shown that the total strain for the pre-cracked SHCC studied here under tensile creep load, is dominated by the "cracking" strain component, accounting for more than 90% of the total strain. This is based on the assumption that the composite between the cracks has the creep compliance as measured for uncracked SHCC. The cracking strain component comprises of the increase in the number of cracks, and the widening of cracks, cf. Eq. (3). The tests performed in this research prove that

these two mechanisms exist, but do not distinguish between their respective contributions. This is a current focus of further research.

5. Conclusions

An investigation of the sources of increased tensile creep of cracked SHCC compared to uncracked SHCC was performed. Three sources of tensile creep of SHCC were identified:

- Matrix creep: the tensile strain increase when a sustained load is applied to uncracked SHCC can be attributed to the creep of the matrix. This has been investigated by Boshoff and Van Zijl [7].
- Time-dependant crack initiation: it was found in this study that one of the reasons for the increase of the tensile creep of cracked SHCC is the further initiation of cracks when a sustained load is applied.
- Time-dependant fibre pull-out: fibres gradually pull-out of the matrix if a sustained load is applied. SHCC cracks become wider with time under a sustained load, which is a direct result of this mechanism.

It was also found that the PVA fibres used in the SHCC in this research do not creep significantly under a sustained load and therefore do not contribute to the tensile creep of this SHCC. The most dominant mechanisms causing the increased tensile creep of pre-cracked SHCC have been shown to be the formation of new cracks and crack widening due to time-dependant fibre pull-out.

Acknowledgements

The first author was supported by a DAAD grant. The support of the South African Ministry of Trade and Industry through the Technology and Human Resources for Industry Programme (THRIP), as well as the industrial partners of the THRIP project SAPERCS is gratefully acknowledged.

References

[1] V.C. Li, S. Wang, C. Wu, Tensile strain-hardening behavior of PVA-ECC, ACI Materials Journal 98 (6) (2001) 483–492.
[2] V.C. Li, C. Wu, S. Wang, A. Ogawa, T. Saito, Interface tailoring for strain-hardening PVA-ECC, ACI Materials Journal 99 (5) (2002) 463–472.
[3] M. Maalej, V.C. Li, Introduction of strain-hardening engineered cementitious composites in design of reinforced concrete flexural members for improved durability, ACI Structural Journal 92 (2) (1995).
[4] V.C. Li, Integrated structural and material design, Material and Structures, vol. 40, RILEM, 2007, pp. 387–396.
[5] S.F.Y. Ahmed, H. Mihashi, A review on durability properties of strain hardening fibre reinforced cementitious composites (SHFRCC), Cement and Concrete Composites, vol. 29, Elsevier, 2007, pp. 365–376.
[6] M. Maalej, S.T. Quek, J. Zhang, Behaviour of Hybrid-Fibre Engineered Cemetitious Composites Subjected to Dynamic Tensile Loading a Projectile Impact, Journal of Materials in Civil Engineering, ASCE, 2005, pp. 143–152.
[7] W.P. Boshoff, G.P.A.G. Van Zijl, Time-dependant response of ECC: Characterisation of creep and rate dependence, Cement and Concrete Research, vol. 37, Elsevier, 2007, pp. 725–734.
[8] W.P. Boshoff, Time-dependant behaviour of ECC, Dissertation, University of Stellenbosch, South Africa, 2007.
[9] H. Stander, Interfacial bond properties for ECC overlay systems, MScEng-thesis, University of Stellenbosch, South Africa, 2007.
[10] W.P. Boshoff, V. Mechtcherine, G.P.A.G. Van Zijl, Characterising the time-dependant behaviour on the single fibre level of SHCC: Part 2: The rate effects on fibre pull-out tests, Cement and Concrete Research 39 (9) (2009) 787–797.
[11] A. Katz, V.C. Li, A Special Technique for Determining the Bond Strength of Carbon Fibers in Cement Matrix by Pullout Test, Journal of Materials Science Letters 15 (1996) 1821–1823.